Partial Differential Equations in Applied Mathematics 8 (2023) 100537

Contents lists available at ScienceDirect

Partial Differential Equations in Applied Mathematics

journal homepage: www.elsevier.com/locate/padiff

Numerous analytical wave solutions to the time-fractional unstable nonlinear Schrödinger equation with beta derivative

Sujoy Devnath [a], Kamruzzaman Khan [b,c,*], M. Ali Akbar [a]

[a] Department of Applied Mathematics, University of Rajshahi, Rajshahi-6205, Bangladesh
[b] Department of Mathematics, Pabna University of Science and Technology, Pabna-6600, Bangladesh
[c] School of Science and Technology, University of New England, Armidale, NSW 2351, Australia

ARTICLE INFO

Keywords:
Solitary wave
Beta derivative
Hamiltonian function
Extended Kudryashov method

ABSTRACT

Fractional nonlinear evolution equations are mathematical representations used to explain a wide range of complex phenomena occurring in nature. By incorporating fractional order viscoelasticity, these equations can accurately depict the intricate behaviour of materials or mediums, requiring fewer parameters compared to classical models. Furthermore, fractional viscoelastic models align with molecular theories and thermodynamics, making them highly compatible. Consequently, the scientific community has shown significant interest in fractional nonlinear evolution equations and their soliton solutions. This study employs the extended Kudryashov method to derive soliton solutions for the time-fractional unstable nonlinear Schrödinger equation, utilizing the Atangana–Baleanu fractional derivative known as the beta derivative. The obtained solitons exhibit various shapes, including V-shaped, periodic, singular periodic, flat kink, and singular bell, under specific conditions. To better understand their physical characteristics, 3D and contour plots are presented by assigning parameter values to certain solutions. Additionally, 2D graphs are generated to observe how the fractional parameter affects the solutions. The Hamiltonian function is determined to further analyse the dynamics of the phase plane. The simulations were conducted using Mathematica and MATLAB software tools. The outcomes of this research contribute to a deeper understanding of the behaviour of fractional nonlinear evolution equations and their soliton solutions, offering insights into the complex dynamics of viscoelastic systems.

1. Introduction

An enormous number of natural phenomena can be described by nonlinear evolution equations (NLEEs). The NLEEs arise in various fields of science and engineering including optics, plasma physics, solid-state physics, fluid dynamics, and so on.[1–4] The fractional-order derivative is a generalization of the derivative of integer order. In many practical situations, fractional nonlinear evolution equations (FNLEEs) are more suitable and general than NLEEs. For illustration, the classical differential relaxation and oscillation equations are the two special cases of fractional differential equation $D_t^\mu u(t) + u(t) - q(t) = 0$, $t > 0$, $0 < \mu \le 2$, and $F = kD_t^\mu x$ which is the generalization of Hooke's model of elasticity, Newton's second law, and Newton's formula for viscosity.[5] The behaviour of viscoelastic food ingredients under stress and relaxation may be modelled mathematically using fractional calculus.[6] Also, the use of fractional differential equation solutions to fit experimental data is a promising technique in the modelling of the change of properties of wires in transport equipment.[7] FNLEEs and their applications in science and engineering are highly essential and, recently, have piqued the attention of many scholars and researchers. To analyse FNLEEs effectively, a precise and well-defined framework for fractional derivatives (FD) is required. Several noteworthy definitions have emerged as prominent choices in this field, including the Caputo FD, Riemann–Liouville (R–L) FD, the conformal fractional derivative,[8] M-fractional derivatives,[9] ABC FD[10] and the beta FD,[11] and others. These definitions provide a solid framework that allows for rigorous investigation and understanding of FNLEEs.

The family of nonlinear Schrodinger equations is used extensively in various applied research domains, such as plasma physics, nonlinear optics, quantum mechanics, metrology, etc. One of them is the time-fractional unstable nonlinear Schrodinger equation (UNLSE) that describes the time evolution of perturbation in the two-layer baroclinic instability and the lossless symmetric two-stream plasma instability.[12,13] The time-fractional unstable nonlinear Schrodinger equation (UNLSE) has the following form[14]:

$$iD_t^\mu q(x,t) + q_{xx}(x,t) + 2\eta\,|q(x,t)|^2\, q(x,t) - 2\gamma q(x,t) = 0, 0 < \mu \le 1, \quad (1.1)$$

where $q(x,t)$ is the complex-valued function that represents the envelope of the wave or the quantum mechanical wave function. η is the coefficient that determines the strength of the nonlinearity in the

* Corresponding author at: Department of Mathematics, Pabna University of Science and Technology, Pabna-6600, Bangladesh.
E-mail address: kkamruzz@une.edu.au (K. Khan).

https://doi.org/10.1016/j.padiff.2023.100537
Received 30 December 2022; Received in revised form 21 June 2023; Accepted 5 July 2023

UNLSE. It affects the interaction between the wave and itself, leading to phenomena such as self-focusing or self-phase modulation. γ is the coefficient that represents the strength of the linear damping or loss term in the NLSE. It accounts for energy dissipation or attenuation of the wave.

The physical motivation and reasoning behind considering the nonlinear Schrödinger equation lie in its broad applicability and relevance to various physical phenomena. The nonlinear Schrödinger equation arises in diverse fields of physics, including optics, quantum mechanics, fluid dynamics, and condensed matter physics, among others.[15] In optics, the nonlinear Schrödinger equation is widely used to study phenomena such as self-focusing, soliton propagation, and optical pulse shaping. It provides a valuable framework for understanding the behaviour of intense laser pulses in nonlinear media, optical fibre communication systems, and nonlinear optical devices.[16]

In quantum mechanics, the nonlinear Schrödinger equation finds applications in Bose–Einstein condensates, where it describes the collective behaviour of ultracold atomic gases.[15] Moreover, the nonlinear Schrödinger equation has implications in fluid dynamics, where it can describe the behaviour of weakly nonlinear waves on the surface of water or in other fluid systems. It provides insights into phenomena such as rogue waves and wave breaking. Overall, the nonlinear Schrödinger equation serves as a versatile mathematical tool for understanding and analysing various physical phenomena in different fields of research, enabling deeper insights into the behaviour of nonlinear waves in complex systems.

A set of methodologies have been successfully developed to achieve the analytical solution for FNLEEs such as the ϕ^6 model expansion technique,[1] the extended hyperbolic function method,[2] the two-variable $(G'/G, 1/G)$-expansion method,[9,17] the tanh–coth method,[18] the enhanced modified simple equation method,[19,20] the Exp-expansion method,[21] the improved Bernoulli sub-equation function method,[22,23] the sine-Gordon function method, the Jacobi elliptic method,[24] the homotopy decomposition method,[25] the Kudryashov method,[26] the generalized Kudryashov method,[27] the extended Kudryashov method,[28] the multiple Exp-function method,[29] hyperbolic function method,[30] first integral and the functional variable strategy,[31] Hirota bilinear method[32,33] and so on. Among the methodologies, the extended Kudryashov method is an effective and straightforward method that takes full advantage of the combination of all solutions of the Riccati and Bernoulli equations.[28] To solve an FNLEE we take the help of homogeneous balance between the highest order derivative and nonlinear term. For this reason, the solutions that come out from this method are in the form of soliton. Soliton is a special type of travelling wave that can travel a long distance without deviation. In the field of analytical solutions for FNLEEs, soliton wave solutions play a crucial role in enhancing our understanding of nonlinear systems and their characteristic features. Researchers have previously attained various soliton shapes, including but not limited to lump-stripe, lump-periodic, breather, bell, anti-bell, kink, periodic, singular and others.[1–5,34] These soliton shapes offer valuable insights into the dynamics of nonlinear systems, allowing for the exploration of their properties, interactions, and stability.[34] In past years, some techniques for extracting the soliton solution of the UNLS equation both for fractional and integer order have been executed. For example, Mousa Ilie et al.[14] implemented the modified Kudryashov method and the sine-Gordon expansion approach in a conformable fractional derivative context. In a conformable fractional derivative sense, Razzaq et al.[35] used an improved auxiliary equation strategy. The authors[36,37] applied the new Jacobi elliptic function rational expansion method, the exponential rational function method, and improved auxiliary equation strategies to solve integer order UNLS equation. The authors[38] utilize extended Jacobi's elliptic expansion functions method to the time-fractional UNLS equation with the truncated M-fractional derivative.

In this article, we will find the soliton solution of the time fractional UNLS equation using the extended Kudryashov method in the frame of beta derivative. To the best of our knowledge, no prior research has used this technique with beta derivative to solve the time fractional UNLS equation.

The leftover article is organized as follows: The definition and properties of the beta derivative are given in Section 2. In Section 3, the key steps of the above-mentioned technique are explained. In Section 4, we apply this technique to Eq. (1.1). In Section 5, Comparisons are discussed. The graphical demonstration and discussion are presented in Section 6. In Section 7, the phase plane is discussed. Finally, in Section 8, we retrieved the conclusions and future directions.

2. Preliminaries of beta derivative

In 2016 Atangana et al.[39] published a new method of fractional derivative in the paper "Analysis of time-fractional Hunter-Saxton equation: a model of nematic liquid crystal" which is well-known as beta derivative or Atangana conformal derivative. The Atangana fractional derivative for the function $\psi(t):\mathbb{R}_+\to\mathbb{R}$ is defined as,[11,39]

$$ {}_0^A D_t^{\mu}\psi(t)=\lim_{\delta\to 0}\frac{\psi\left(t+\delta\left(t+\frac{1}{\Gamma\mu}\right)^{1-\mu}\right)-\psi(t)}{\delta}, 0<\mu\le 1. \tag{2.1}$$

Using the transformation $\delta=\xi\left(\mathrm{t}+\frac{1}{\Gamma\mu}\right)^{\mu-1}$, $\xi\to 0$ as $\delta\to 0$ (2.1) can be reduced to the following form:[40]

$$ {}_0^A D_t^{\mu}\psi(t)=\left(t+\frac{1}{\Gamma\mu}\right)^{1-\mu}\lim_{\xi\to 0}\frac{\psi(t+\xi)-\psi(t)}{\xi}=\left(t+\frac{1}{\Gamma\mu}\right)^{1-\mu}\frac{d\psi(t)}{dt}. \tag{2.2}$$

This definition satisfies all the fundamental properties of conventional calculus. Assuming that functions $\psi\neq 0$ and $\Phi\neq 0$ are differentiable with $\mu\in(0,1]$. Then the following five relations hold.[41]

i. ${}_0^A D_t^{\mu} C=0$.
ii. ${}_0^A D_t^{\mu}\left[c_1\psi(t)+c_2\Phi(t)\right]=c_1{}_0^A D_t^{\mu}\psi(t)+c_2{}_0^A D_t^{\mu}\Phi(t)$.
iii. ${}_0^A D_t^{\mu}\{\psi(t)\Phi(t)\}=\psi(t){}_0^A D_t^{\mu}\Phi(t)+\Phi(t){}_0^A D_t^{\mu}\psi(t)$.
iv. ${}_0^A D_t^{\mu}\frac{\psi(t)}{\Phi(t)}=\frac{\Phi(t){}_0^A D_t^{\mu}\psi(t)-\psi(t){}_0^A D_t^{\mu}\Phi(t)}{\Phi^2(t)}$.
v. ${}_0^A D_t^{\mu}\psi(\Phi(t))=\frac{d\psi(\Phi(t))}{d\Phi(t)}{}_0^A D_t^{\mu}\Phi(t)$.

The proof of the above relations:

Theorem 1. *The beta derivative of a constant function is zero, i.e.* ${}_0^A D_t^{\mu} k=0$.[42]

Proof. Consider a constant function $\psi(t)=k$, for any values of t.

Now, μ $(0<\mu\le 1)$ times beta derivative of ψ is defined as in Eq. (2.1)

$$ {}_0^A D_t^{\mu}\psi(t)=\lim_{\delta\to 0}\frac{\psi\left(t+\delta\left(t+\frac{1}{\Gamma\mu}\right)^{1-\mu}\right)-\psi(t)}{\delta}.$$

$$ {}_0^A D_t^{\mu}\psi(t)=\lim_{\delta\to 0}\frac{k-k}{\delta}=0.$$

Therefore, the beta derivative of a constant function is zero.

Theorem 2. *The beta derivative of the product of a constant and a function is the product of the constant and the beta derivative of the function,*[42] *i.e.,* ${}_0^A D_t^{\mu}\psi(t)=k{}_0^A D\Phi(t)$.

Proof. Consider a function $\psi:\mathbb{R}_+\to\mathbb{R}$ defined as $\psi(t)=k\Phi(t)$ where k is a constant. The beta derivative of ψ is

$$ {}_0^A D_t^{\mu}\psi(t)=\lim_{\delta\to 0}\frac{\psi\left(t+\delta\left(t+\frac{1}{\Gamma\mu}\right)^{1-\mu}\right)-\psi(t)}{\delta} 0<\mu\le 1.$$

$$ {}_0^A D_t^{\mu}\psi(t)=\lim_{\delta\to 0}\frac{k\Phi\left(t+\delta\left(t+\frac{1}{\Gamma\mu}\right)^{1-\mu}\right)-k\Phi(t)}{\delta}.$$

$$ {}_0^A D_t^\mu \psi(t) = k \lim_{\delta\to 0} \frac{\Phi\left(t+\delta\left(t+\frac{1}{\Gamma\mu}\right)^{1-\mu}\right)-\Phi(t)}{\delta}. $$

$$ {}_0^A D_t^\mu \psi(t) = k\, {}_0^A D\Phi(t). $$

Hence, the beta derivative of the product of a constant and a function is the product of the constant and the beta derivative of the function.

Theorem 3. *The beta derivative of the product of the two functions is equal to the sum of the product of the first function and beta derivative of the second function and the product of the second function and beta derivative of the first function,*[42] *i.e.*

$$ {}_0^A D_t^\mu \{\psi(t)\,\Omega(t)\} = \Omega(t)\, {}_0^A D_t \psi(t) + \psi(t)\, {}_0^A D_t^\mu \Omega(t). $$

Proof. Consider a function $\Phi : \mathbb{R}_+ \to \mathbb{R}$ defined as $\Phi(t) = \Omega(t)\,\psi(t)$. The beta derivative of function ψ is

$$ \begin{aligned} {}_0^A D_t^\mu \Phi(t) &= \lim_{\delta\to 0} \frac{\Phi\left(t+\delta\left(t+\frac{1}{\Gamma\mu}\right)^{1-\mu}\right)-\Phi(t)}{\delta}, \quad 0<\mu\le 1 \\ &= \lim_{\delta\to 0} \frac{1}{\delta}\left[\Omega\left(t+\delta\left(t+\frac{1}{\Gamma\mu}\right)^{1-\mu}\right)\psi\left(t+\delta\left(t+\frac{1}{\Gamma\mu}\right)^{1-\mu}\right)-\Omega(t)\,\psi(t)\right] \\ &= \lim_{\delta\to 0} \frac{1}{\delta}\left[\Omega\left(t+\delta\left(t+\frac{1}{\Gamma\mu}\right)^{1-\mu}\right)\psi\left(t+\delta\left(t+\frac{1}{\Gamma\mu}\right)^{1-\mu}\right)-\Omega(t)\,\psi(t)\right. \\ &\quad \left. -\,\Omega\left(t+\delta\left(t+\frac{1}{\Gamma\mu}\right)^{1-\mu}\right)\psi(t)+\Omega\left(t+\delta\left(t+\frac{1}{\Gamma\mu}\right)^{1-\mu}\right)\psi(t)\right] \\ &= \lim_{\delta\to 0}\Omega\left(t+\delta\left(t+\frac{1}{\Gamma\mu}\right)^{1-\mu}\right)\lim_{\delta\to 0}\frac{\psi\left(t+\delta\left(t+\frac{1}{\Gamma\mu}\right)^{1-\mu}\right)-\psi(t)}{\delta} \\ &\quad +\psi(t)\lim_{\delta\to 0}\frac{\Omega\left(t+\delta\left(t+\frac{1}{\Gamma\mu}\right)^{1-\mu}\right)-\Omega(t)}{\delta} \\ &= \Omega(t)\lim_{\delta\to 0}\frac{\psi\left(t+\delta\left(t+\frac{1}{\Gamma\mu}\right)^{1-\mu}\right)-\psi(t)}{\delta} \\ &\quad +\psi(t)\lim_{\delta\to 0}\frac{\Omega\left(t+\delta\left(t+\frac{1}{\Gamma\mu}\right)^{1-\mu}\right)-\Omega(t)}{\delta} \end{aligned} $$

$$ {}_0^A D_t^\mu \Phi(t) = {}_0^A D_t^\mu\{\psi(t)\,\Omega(t)\} = \Omega(t)\, {}_0^A D_t \psi(t) + \psi(t)\, {}_0^A D_t^\mu \Omega(t). $$

Therefore, the beta derivative of $\Omega(t)\Phi(t)$ is equal to the sum of the product of $\Omega(t)$ and the beta derivative of $\psi(t)$ and the product of $\psi(t)$ and beta derivative of the $\Omega(t)$.

Theorem 4. *The beta fractional derivative of a composite function, $\psi(\Phi(t))$ is equal to the product of the classical derivative of ψ with respect to $\Phi(t)$ and the beta derivative of $\Phi(t)$ with respect to t.*[41]

Let a composite function $Z : \mathbb{R}_+ \to \mathbb{R}$ defined as $Z = \psi(\Phi(t))$. This can be written as $Z = \psi(\chi)$ where $\chi = \Phi(t)$. Also, assume that both the functions ψ andϕ are differentiable. The beta derivative of function Z is

$$ \begin{aligned} {}_0^A D_t^\mu Z &= {}_0^A D_t^\mu \psi\{\Phi(t)\} \\ &= \lim_{\delta\to 0}\frac{\psi\left\{\Phi\left(t+\delta\left(t+\frac{1}{\Gamma\mu}\right)^{1-\mu}\right)\right\}-\psi\{\Phi(t)\}}{\delta}, \quad 0<\mu\le 1 \\ &= \lim_{\delta\to 0}\frac{\psi\left\{\Phi\left(t+\delta\left(t+\frac{1}{\Gamma\mu}\right)^{1-\mu}\right)\right\}-\psi\{\Phi(t)\}}{\Phi\left(t+\delta\left(t+\frac{1}{\Gamma\mu}\right)^{1-\mu}\right)-\Phi(t)} \\ &\quad \cdot\frac{\Phi\left(t+\delta\left(t+\frac{1}{\Gamma\mu}\right)^{1-\mu}\right)-\Phi(t)}{\delta} \\ &= \lim_{\delta\to 0}\frac{\psi\left\{\Phi\left(t+\delta\left(t+\frac{1}{\Gamma\mu}\right)^{1-\mu}\right)\right\}-\psi\{\Phi(t)\}}{\Phi\left(t+\delta\left(t+\frac{1}{\Gamma\mu}\right)^{1-\mu}\right)-\Phi(t)} \\ &\quad \cdot\lim_{\delta\to 0}\frac{\Phi\left(t+\delta\left(t+\frac{1}{\Gamma\mu}\right)^{1-\mu}\right)-\Phi(t)}{\delta} \\ &= \lim_{\delta\to 0}\frac{\psi\left\{\Phi\left(t+\delta\left(t+\frac{1}{\Gamma\mu}\right)^{1-\mu}\right)\right\}-\psi\{\Phi(t)\}}{\Phi\left(t+\delta\left(t+\frac{1}{\Gamma\mu}\right)^{1-\mu}\right)-\Phi(t)}\cdot {}_0^A D_t^\mu \Phi(t) \end{aligned} $$

[by Eq. (2.1)]

Setting $\left(t+\delta\left(t+\frac{1}{\Gamma\mu}\right)^{1-\mu}\right) = h, h\to 0$ as $\delta\to 0$,

$$ = \lim_{h\to 0}\frac{\psi\{\Phi(t+h)\}-\psi\{\Phi(t)\}}{\Phi(t+h)-\Phi(t)}\cdot {}_0^A D_t^\mu \Phi(t) $$

Consider,

Considered, $\Phi(t+h)-\Phi(t) = k, k\to 0$ as $h\to 0$,

$$ \begin{aligned} &= \lim_{h\to 0}\frac{\psi\{\phi(t)+k\}-\psi\{\Phi(t)\}}{k}\cdot {}_0^A D_t^\mu \Phi(t) \\ &= \frac{d}{d\phi(t)}\psi\{\Phi(t)\}\cdot {}_0^A D_t^\mu \Phi(t) \end{aligned} $$

Therefore, ${}_0^A D_t^\mu \psi(\phi(t)) = \dfrac{d\psi(\phi(t))}{d\Phi(t)}\, {}_0^A D_t^\mu \Phi(t)$.

3. Overview of the extended Kudryashov method

In this part of the article, we will briefly discuss the working procedure of the EK method. We split the entire procedure of this method into five key steps as follows:[28]

Assume the following space–time fractional non-linear evolution equation (FNLEEs) with function Z (real or complex) of the independent variables $X = (x_1, x_2, x_3, \dots, t)$

$$ Q(Z, Z_{x_1} \dots D_t^\mu Z, D_{x_2}^\mu Z, D_{x_3}^\mu Z, \dots, D_t^{2\mu} Z, D_{x_2}^{2\mu} Z, D_{tx_2}^{2\mu} Z, \dots) = 0 \tag{3.1} $$

where Q is a polynomial in Z and its various partial fractional derivative involving the highest-order derivative and nonlinear terms.

$D_t^\mu = \dfrac{d^\mu}{dt^\mu}, D_{x_2}^\mu = \dfrac{d^\mu}{dx_2^\mu}, D_t^{2\mu} = \dfrac{d^\mu}{dt^\mu}\dfrac{d^\mu}{dt^\mu},$

$D_{x_2 t}^{2\mu} = \dfrac{d^\mu}{dx_2^\mu}\dfrac{d^\mu}{dt^\mu}, \dots$ denote the fractional beta derivative operator.

Step 1. The travelling wave transformation is a combination of space and time. For the real function, the transformation is

$$ Z(x_1, x_2, x_3, \dots, t) = u(\rho), \tag{3.2} $$

$$ \rho = \frac{k_1}{\mu}\left(t+\frac{1}{\Gamma\mu}\right)^\mu + \frac{k_2}{\mu}\left(x_2+\frac{1}{\Gamma\mu}\right)^\mu + \frac{k_3}{\mu}\left(x_3+\frac{1}{\Gamma\mu}\right)^\mu + \dots + k_p x_1 $$

and for the complex-valued function, the transformation is

$$ Z(x_1, x_2, x_3, \dots, t) = u(\rho)\, e^{i\theta}, \tag{3.3} $$

$$ \rho = \frac{k_1}{\mu}\left(t+\frac{1}{\Gamma\mu}\right)^\mu + \frac{k_2}{\mu}\left(x_2+\frac{1}{\Gamma\mu}\right)^\mu + \frac{k_3}{\mu}\left(x_3+\frac{1}{\Gamma\mu}\right)^\mu + \dots + k_p x_1 $$

and

$$ \theta = \frac{\eta_1}{\mu}\left(t+\frac{1}{\Gamma\mu}\right)^\mu + \frac{\eta_2}{\mu}\left(x_2+\frac{1}{\Gamma\mu}\right)^\mu + \frac{\eta_3}{\mu}\left(x_3+\frac{1}{\Gamma\mu}\right)^\mu + \dots + \eta_p x_1, $$

where $k_1, k_2, k_3 \dots k_p, \eta_1, \eta_2, \eta_3, \dots \eta_p$ are arbitrary constant.

Eq. (3.2) or Eq. (3.3) converts Eq. (3.1) to the following nonlinear ordinary differential equation

$$Q\left(z, z', z'', z''', \dots\right) = 0. \tag{3.4}$$

Step 2: The solution to Eq. (3.4) can be written in the following form,

$$u(\rho) = A_0 + \sum_{l=1}^{N}\sum_{i+k=l} A_{ik}\Phi(\rho)^{i}\psi(\rho)^{k} + \sum_{l=1}^{N}\sum_{i+k=l}\frac{B_{ik}}{\Phi(\rho)^{i}\psi(\rho)^{k}}, \tag{3.5}$$

where the constants $A_0, A_{ik}, B_{ik}(i,k = 1,2,3\dots N)$ to be determined. The function $\Phi(\rho)$ and $\psi(\rho)$ satisfies the Riccati and Bernoulli equation.

The Bernoulli differential equation,

$$\psi'(\rho) = S_0 + S_1\psi(\rho) + S_2\psi^2(\rho), \tag{3.6}$$

has the following solutions,

$$\psi(\rho) = \begin{cases} \frac{-S_1}{2S_2} - \frac{\sqrt{\alpha}}{2S_2}\tanh\left(\frac{\sqrt{\alpha}}{2}\rho + \beta\right), & \alpha > 0 \\ \frac{-S_1}{2S_2} - \frac{\sqrt{\alpha}}{2S_2}\coth\left(\frac{\sqrt{\alpha}}{2}\rho + \beta\right), & \alpha > 0 \\ \frac{-S_1}{2S_2} + \frac{\sqrt{-\alpha}}{2S_2}\tan\left(\frac{\sqrt{-\alpha}}{2}\rho + \beta\right), & \alpha < 0 \\ \frac{-S_1}{2S_2} - \frac{\sqrt{-\alpha}}{2S_2}\cot\left(\frac{\sqrt{-\alpha}}{2}\rho + \beta\right), & \alpha < 0 \\ \frac{-S_1}{2S_2} + \frac{-1}{S_2\rho+\beta}, & \alpha = 0. \end{cases} \tag{3.7}$$

where $\alpha = S_1^2 - 4S_0S_2$ and β is an arbitrary real constant.

The Riccati differential equation,

$$\Phi'(\rho) = -R_1\Phi(\rho) + R_2\Phi^2(\rho), \tag{3.8}$$

has the following solutions,

$$\Phi(\rho) = \begin{cases} \frac{-1}{R_2\rho+\beta}, & R_1 = 0 \\ \frac{R_1}{R_2+R_1 exp(R_1\rho+\beta)}, & R_1 \neq 0. \end{cases} \tag{3.9}$$

The coefficients S_0, S_1, S_2 in Eq. (3.6) and R_1, R_2 in Eq. (3.9) are constant coefficients of the Bernoulli and Riccati equation.

Step 3: The value of N in Eq. (3.5) is most important for the soliton solutions of Eq. (3.4). In the case of soliton solution the highest order derivative balance with the nonlinear terms of Eq. (3.4), which provides the positive integer value of N.

Step 4: A polynomial of $\Phi(\rho)\psi(\rho)$ is attained after inserting (3.5) into (3.4) along with (3.6) and (3.8). Then we construct an algebraic system of equations by collecting all the coefficients of $\Phi^{l}(\rho)\Psi^{m}(\rho)$, (l, m = 1,2, 3, …) from the polynomial and equating them to zero.

Step 5: With the assistance of Mathematica, this difficult algebraic system of equations can be solved for $A_0, A_{ik}, B_{ik}\,(i,k = 0,1,2,3,\dots,N)$. Substituting the values of the coefficients into solution (3.5) together with Eq. (3.7) and Eq. (3.9), a list of solutions to the FNLEE Eq. (3.1) can be obtained.

4. Solutions analysis

Eq. (1.1) is transformed into a nonlinear differential equation

$$e^{i\theta}\left(-\left(p^2 + 2\gamma + v\right)u(\rho) + 2\eta u(\rho)^3 + i\left(2kp + \omega\right)u'(\rho) + k^2u''(\rho)\right) = 0 \tag{4.1}$$

by performing the travelling wave transformation $q(x,t) = u(\rho)e^{i\theta(x,t)}$, $\rho = kx - \frac{\omega}{\mu}(t + \frac{1}{\Gamma\mu})^{\mu}$ and $\theta = px + \frac{v}{\alpha}(t + \frac{1}{\Gamma\mu})^{\mu}$

where the real function $u(\rho)$ and $\theta(x,t)$ are the shape and the phase component of the soliton, p represents the frequency, v is the wave number, and ω is the velocity of the soliton.

The real and imaginary parts of (4.1) provide

$$-\left(p^2 + 2\gamma + v\right)u(\rho) + 2\eta u(\rho)^3 + k^2u''(\rho) = 0 \tag{4.2}$$

$$\text{and } \omega = 2kp. \tag{4.3}$$

In Eq. (4.2), if we balance $u''(\rho)$ with $u(\rho)^3$, then we attain $N = 2$. Consequently, Eq. (4.2) has the solution in following form,

$$u(\rho) = A_0 + A_{1,0}\phi(\rho) + A_{0,1}\psi(\rho) + \frac{B_{1,0}}{\phi(\rho)} + \frac{B_{0,1}}{\psi(\rho)}. \tag{4.4}$$

The following sets of the coefficient value along with v are attained according to the method.

Set 1: $A_0 = \mp\frac{ikR_1}{2\sqrt{\eta}}, A_{1,0} = \pm\frac{ikR_2}{\sqrt{\eta}}, A_{0,1} = B_{1,0} = B_{0,1} = 0, v = \frac{1}{2}(-2p^2 - 4\gamma - k^2R_1^2)$.

Set 2: $A_0 = \pm\frac{ikS_1}{2\sqrt{\eta}}, A_{1,0} = 0, A_{0,1} = \pm\frac{ikS_2}{\sqrt{\eta}}, B_{1,0} = B_{0,1} = 0, v = \frac{1}{2}(-2p^2 - 4\gamma - k^2S_1^2 + 4k^2S_0S_2)$.

Set 3: $A_0 = \pm\frac{ikS_1}{2\sqrt{\eta}}, A_{1,0} = A_{0,1} = B_{1,0} = 0, B_{0,1} = \pm\frac{ikS_0}{\sqrt{\eta}}, v = \frac{1}{2}(-2p^2 - 4\gamma - k^2S_1^2 + 4k^2S_0S_2)$.

Solution type 1.

Soliton solutions of (1.1) corresponding to set 1,

$$q(x,t) = \pm\frac{ikR_2e^{i(px+\frac{v}{\alpha}\left(t+\frac{1}{\Gamma\mu}\right)^{\mu})}}{\sqrt{\eta}(\beta+\rho R_2)}, R_1 = 0 \tag{4.5}$$

$$q(x,t) = \frac{ikR_1}{2\sqrt{\eta}}e^{e^{i(px+\frac{v}{\alpha}\left(t+\frac{1}{\Gamma\mu}\right)^{\mu})}}(1 - \frac{2R_2}{R_1e^{\beta+\rho R_1} + R_2}), R_1 \neq 0. \tag{4.6}$$

After performing some simplification, solution in Eq. (4.6) reduces to

$$q(x,t) = \pm\frac{ikR_1e^{ipx+\frac{v}{\alpha}\left(t+\frac{1}{\Gamma\mu}\right)^{\mu}}}{2\sqrt{\eta}} \times\left(1 - \frac{2R_2\left(Cosh\left[\frac{1}{2}\left(\beta+\rho R_1\right)\right] - Sinh\left[\frac{1}{2}\left(\beta+\rho R_1\right)\right]\right)}{\left(R_1+R_2\right)Cosh\left[\frac{1}{2}\left(\beta+\rho R_1\right)\right] + \left(R_1-R_2\right)Sinh\left[\frac{1}{2}\left(\beta+\rho R_1\right)\right]}\right), R_1 \neq 0. \tag{4.7}$$

Some special cases of the solution in Eq. (4.7)

when $R_1 = R_2 \neq 0$,

$$q(x,t) = \pm\frac{ikR_1}{2\sqrt{\eta}}e^{e^{ipx+\frac{v}{\alpha}\left(t+\frac{1}{\Gamma\mu}\right)^{\mu}}}\tanh\left(\frac{1}{2}\left(\beta+\rho R_1\right)\right), \tag{4.8}$$

when $R_1 = 4, R_2 = 1$,

$$q(x,t) = \pm\frac{2ike^{ipx+\frac{v}{\alpha}\left(t+\frac{1}{\Gamma\mu}\right)^{\mu}}}{2\sqrt{\eta}}\left(1 - \frac{2\left(cosh\left[\frac{1}{2}(\beta+4\rho)\right] - sinh\left[\frac{1}{2}(\beta+4\rho)\right]\right)}{4cosh\left[\frac{1}{2}(\beta+4\rho)\right] + 3sinh\left[\frac{1}{2}(\beta+4\rho)\right]}\right), \tag{4.9}$$

when $R_1 = 3,\ R_2 = 1$,

$$q(x,t) = \pm\frac{3ik}{2\sqrt{\eta}}e^{e^{ipx+\frac{v}{\alpha}\left(t+\frac{1}{\Gamma\mu}\right)^{\mu}}}\left(\frac{cosh\left[\frac{1}{2}(\beta+3\rho)\right] + 2Sinh\left[\frac{1}{2}(\beta+3\rho)\right]}{2cosh\left[\frac{1}{2}(\beta+3\rho)\right] + Sinh\left[\frac{1}{2}(\beta+3\rho)\right]}\right), \tag{4.10}$$

where, $v = \frac{1}{2}(-2p^2 - 4\gamma - k^2R_1^2)$, $\rho = kx - \frac{2kp}{\mu}\left(t + \frac{1}{\Gamma\mu}\right)^{\mu}$.

Solution type 2

Soliton solutions of (1.1) corresponding to Set 2

$$q(x,t) = \frac{\pm ie^{i(px+\frac{v}{\alpha}\left(t+\frac{1}{\Gamma\mu}\right)^{\mu})}k\sqrt{\alpha}tanh[\beta + \frac{1}{2}(kx - \frac{2kp}{\mu}(t+\frac{1}{\Gamma\mu})^{\mu})\sqrt{\alpha}]}{2\sqrt{\eta}}, \alpha > 0, \tag{4.11}$$

$$q(x,t) = \frac{\mp ik\sqrt{\alpha}e^{i(px+\frac{v}{\alpha}\left(t+\frac{1}{\Gamma\mu}\right)^{\mu})}coth[\beta + \frac{1}{2}(kx - \frac{2kp}{\mu}\left(t+\frac{1}{\Gamma\mu}\right)^{\mu})\sqrt{\alpha}]}{2\sqrt{\eta}}, \alpha > 0, \tag{4.12}$$

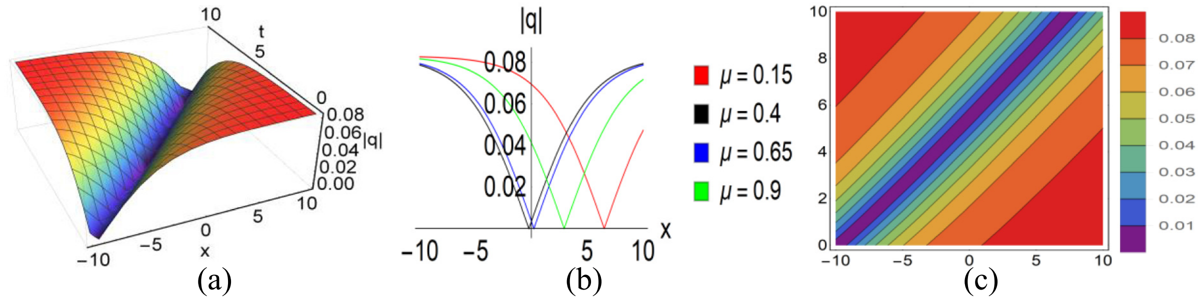

Fig. 1. (a) 3D plot, (b) 2D plot at $t = 7$, (c) contour plot of the absolute part of the solution (4.6).

$$q(x,t) = \frac{\pm ik\sqrt{-\alpha}e^{i(px+\frac{\nu}{\alpha}\left(t+\frac{1}{\Gamma\mu}\right)^{\mu})}\tan[\beta+\frac{1}{2}(kx-\frac{2kp}{\mu}(t+\frac{1}{\Gamma\mu})^{\mu})\sqrt{-\alpha}]}{2\sqrt{\eta}}, \alpha<0, \tag{4.13}$$

$$q(x,t) = \frac{\mp ik\sqrt{-\alpha}e^{ipx+\frac{\nu}{\alpha}(t+\frac{1}{\Gamma\mu})^{\mu}}\cot[\beta+\frac{1}{2}(kx-\frac{2kp}{\mu}(t+\frac{1}{\Gamma\mu})^{\mu})\sqrt{-\alpha}]}{2\sqrt{\eta}}, \alpha<0, \tag{4.14}$$

$$q(x,t) = \frac{ikS_2 e^{ipx+\frac{\nu}{\alpha}(t+\frac{1}{\Gamma\mu})^{\mu}}}{\sqrt{\eta}(\beta+(kx-\frac{2kp}{\mu}(t+\frac{1}{\Gamma\mu})^{\mu})S_2)}, \alpha=0, \tag{4.15}$$

where $\nu = \frac{1}{2}(-2p^2 - 4\gamma - k^2\alpha)$, $\alpha = S_1^2 - 4S_0S_2$.

Solution type 3

Soliton solutions of (1.1) corresponding to Set 3

$$q(x,t) = \frac{\pm ike^{i\left(px+\frac{\nu}{\alpha}\left(t+\frac{1}{\Gamma\mu}\right)^{\mu}\right)}\left(\alpha+\sqrt{\alpha}S_1\, tanh\left[\beta+\frac{1}{2}\left(kx-\frac{2kp}{\mu}\left(t+\frac{1}{\Gamma\mu}\right)^{\mu}\right)\sqrt{\alpha}\right]\right)}{2\sqrt{\eta}\left(S_1+\sqrt{\alpha}tanh\left[\beta+\frac{1}{2}\left(kx-\frac{2kp}{\mu}\left(t+\frac{1}{\Gamma\mu}\right)^{\mu}\right)\sqrt{\alpha}\right]\right)}, \alpha>0, \tag{4.16}$$

$$q(x,t) = \frac{\pm ike^{i\left(px+\frac{\nu}{\alpha}\left(t+\frac{1}{\Gamma\mu}\right)^{\mu}\right)}\left(\alpha-\sqrt{\alpha}S_1 coth\left[\beta+\frac{1}{2}\left(kx-\frac{2kp}{\mu}\left(t+\frac{1}{\Gamma\mu}\right)^{\mu}\right)\sqrt{\alpha}\right]\right)}{2\sqrt{\eta}\left(S_1+\sqrt{\alpha}coth\left[\beta+\frac{1}{2}\left(kx-\frac{2kp}{\mu}\left(t+\frac{1}{\Gamma\mu}\right)^{\mu}\right)\sqrt{\alpha}\right]\right)}, \alpha>0, \tag{4.17}$$

$$q(x,t) = \frac{\pm ike^{i\left(px+\frac{\nu}{\alpha}\left(t+\frac{1}{\Gamma\mu}\right)^{\mu}\right)}\left(\alpha-S_1 tan\left[\beta+\frac{1}{2}\left(kx-\frac{2kp}{\mu}\left(t+\frac{1}{\Gamma\mu}\right)^{\mu}\right)\sqrt{-\alpha}\right]\sqrt{-\alpha}\right)}{2\sqrt{\eta}\left(S_1-tan\left[\beta+\frac{1}{2}\left(kx-\frac{2kp}{\mu}\left(t+\frac{1}{\Gamma\mu}\right)^{\mu}\right)\sqrt{-\alpha}\right]\sqrt{-\alpha}\right)}, \alpha<0, \tag{4.18}$$

$$q(x,t) = \frac{\pm ike^{i(px+\frac{\nu}{\alpha}\left(t+\frac{1}{\Gamma\mu}\right)^{\mu})}(\alpha+S_1 cot\left[\beta+\frac{1}{2}\left(kx-\frac{2kp}{\mu}\left(t+\frac{1}{\Gamma\mu}\right)^{\mu}\right)\sqrt{-\alpha}\right]\sqrt{-\alpha})}{2\sqrt{\eta}(S_1+cot[\beta+\frac{1}{2}\left(kx-\frac{2kp}{\mu}\left(t+\frac{1}{\Gamma\mu}\right)^{\mu}\right)\sqrt{-\alpha}]\sqrt{-\alpha})}, \alpha<0, \tag{4.19}$$

$$q(x,t) = \pm\frac{ike^{i\left(px+\frac{\nu}{\alpha}\left(t+\frac{1}{\Gamma\mu}\right)^{\mu}\right)}}{2\sqrt{\eta}}(S_1-\frac{2S_0}{\frac{S_1}{2S_2}+\frac{1}{\beta+\left(kx-\frac{2kp}{\mu}\left(t+\frac{1}{\Gamma\mu}\right)^{\mu}\right)S_2}}), \alpha=0, \tag{4.20}$$

where $\nu = \frac{1}{2}(-2p^2 - 4\gamma - k^2\alpha)$, $\alpha = S_1^2 - 4S_0S_2$.

5. Comparisons

The extended Kudryashov method and the He's semi-inverse method are two distinct approaches used to analyse equations in mathematical physics, each with its characteristics and advantages. Now we will compare the extended Kudryashov method with the He's semi-inverse method,[43] through the solutions of the time-fractional unstable nonlinear Schrödinger equation. Wang and Xu investigated the time-fractional unstable nonlinear Schrödinger equation by employing the He's semi-inverse method in their research and explored only one solution.[43] Nevertheless, in our current paper, we have utilized the extended Kudryashov method and discovered sixteen solutions expressed in hyperbolic, trigonometric, and exponential functions. The solutions we obtained in our study differ from those presented by Wang and Xu.

6. Graphical representations and discussion

The soliton solutions with specific parameter values are depicted in this section using three-dimensional (3D), two-dimensional (2D), and contour plots within the range $-10 \le x \le 10$, $0 \le t \le 10$. The effects of the fractional parameter on solutions will be investigated using 2D plots.

The absolute part of the solution (4.6) is exhibited for $p = 1, k = 0.16, \mu = 0.9, \eta = 5, \beta = 5, R_1 = 2.32, R_2 = 5$ in Fig. 1. This is a V-shaped soliton and propagates with a velocity of 0.32. The 2D graph is plotted for four distinct fractional parameter (μ) values: 0.15, 0.40, 0.65, and 0.90.

The imaginary part of the solution (4.6) exhibits periodic soliton for $p = 0.91$, $k = 0.23$, $\mu = 0.95$, $\gamma = 0.1$, $\eta = 1.87, \beta = 5$, $R_1 = 3$, $R_2 = 4$ in Fig. 2. The 2D graph is drawn for four different values of fractional parameter, $\mu = 0.15$, 0.40, 0.65, and 0.90. This soliton moves with a velocity of 0.42.

The real part of the solution (4.6) is exhibited for $p = 1.155, k = 0.36, \mu = 0.6, \eta = 1.87, \beta = -5, R_1 = 4, R_2 = 3.8, \gamma = 0.1$ in Fig. 3. The 2D graph is drawn for three particular values of fractional parameter, $\mu = 0.1$, 0.5, and 0.9. This is a periodic soliton and moves with a velocity of 0.83.

The absolute part of the solution (4.11) exhibits a flat kink-shaped soliton for $p = 1.92$, $k = 2.19$, $\mu = 0.8$, $\eta = 0.2$, $\beta = 2.5$, $\alpha = 0.001$ in Fig. 4. The 2D graph is plotted for four distinct fractional parameter (μ) values: $0.1, 0.4, 0.7$, and 1.0. This soliton propagates at the velocity of 8.4.

The imaginary part of the solution (4.11) is exhibited for $p = 0.62$, $k = 0.47$, $\mu = 0.98$, $\eta = 4.5$, $\beta = -2.4$, $\alpha = 1.28$ in Fig. 5. The 2D graph is plotted for four distinct fractional parameter (μ) values: $0.22, 0.57$, and 0.92.

The real part of the solution (4.11) is exhibited for $p = 1.43$, $k = 0.725$, $\mu = 0.89$, $\eta = 4.5$, $\beta = 5$, $\alpha = 2.98$, $\gamma = -1.4$ in Fig. 6. The 2D graph is drawn for three different values of fractional parameter, $\mu = 0.2, 0.6$, and 1.0.

The real part of the solution (4.20) is exhibited for $p = 0.58$, $k = 5$, $\mu = 0.85$, $\eta = 0.1$, $\beta = 1$, $S_0 = 1$, $S_1 = 2$, $S_2 = 1$ in Fig. 7. The 2D graph is drawn for four distinct fractional values of the parameter (μ): $0.10, 0.50$, and 0.90. It is clear from Fig. 7(b) that the wave amplitude increases with the increase of the values of the fractional parameter μ.

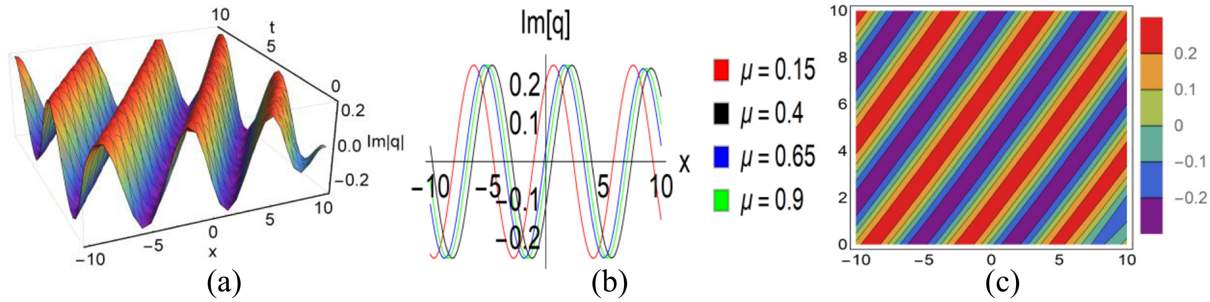

Fig. 2. (a) 3D plot, (b) 2D plot at $t = 3$, (c) contour plot of the imaginary part of the solution (4.6).

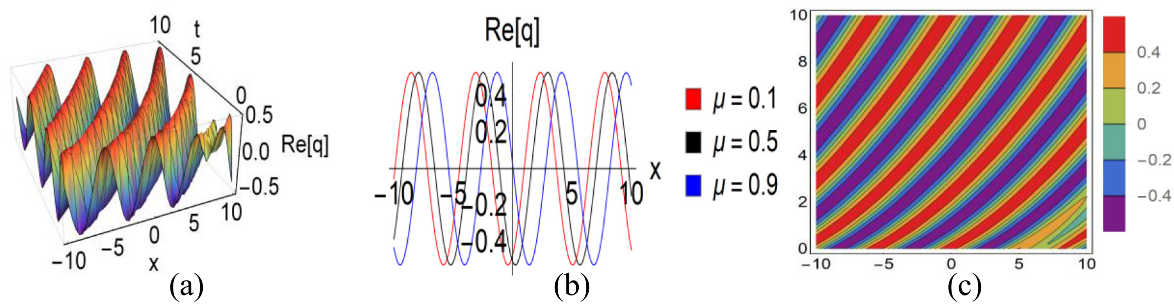

Fig. 3. (a) 3D plot, (b) 2D plot at $t = 4$, (c) contour plot of the real part of the solution (4.6).

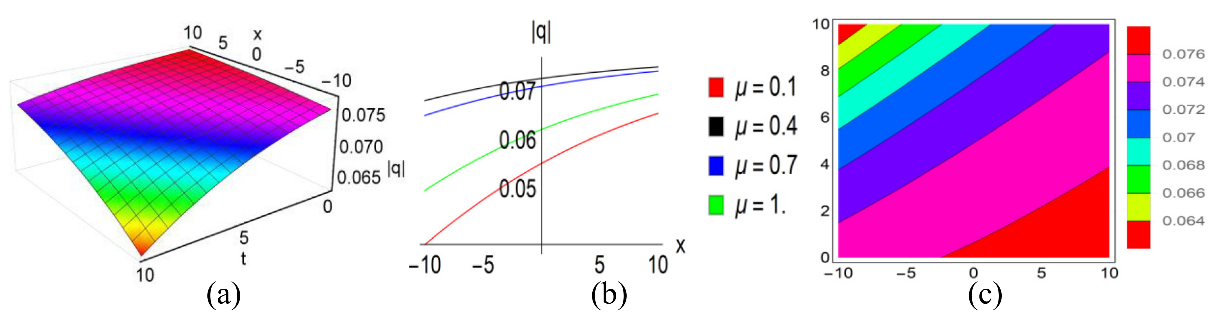

Fig. 4. (a) 3D plot, (b) 2D plot at $t = 10$, (c) contour plot of the absolute part of the solution (4.11).

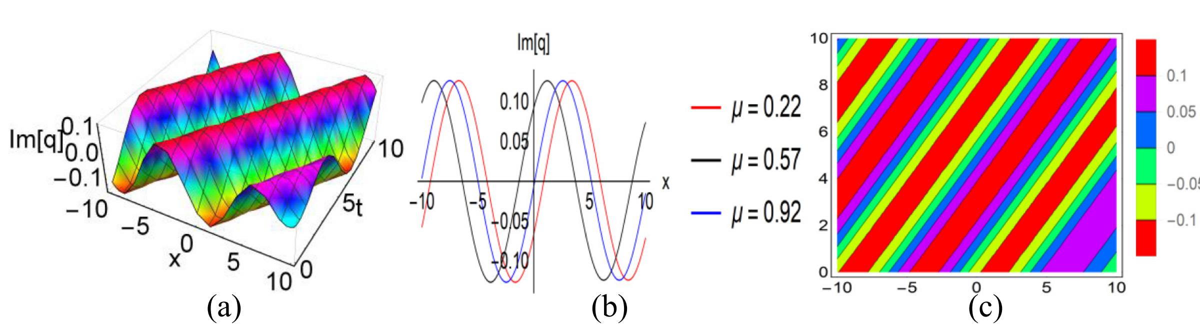

Fig. 5. (a) 3D plot, (b) 2D plot at $t = 5$, (c) contour plot of the imaginary part of the solution (4.11).

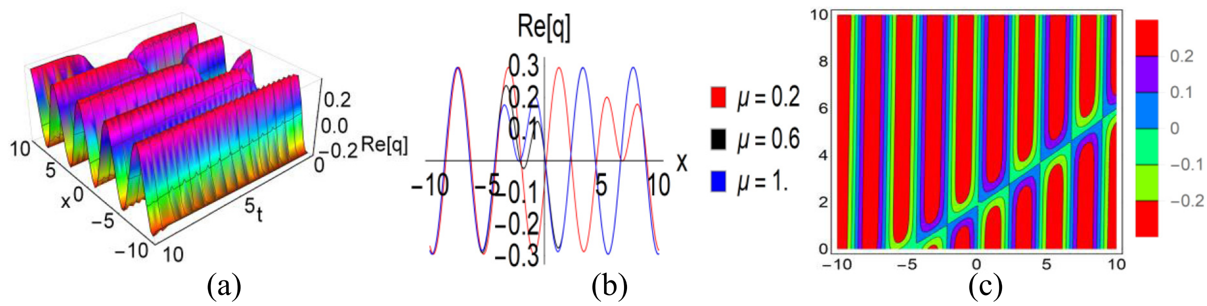

Fig. 6. (a) 3D plot, (b) 2D plot at $t = 4$, (c) contour plot of the real part of the solution (4.11).

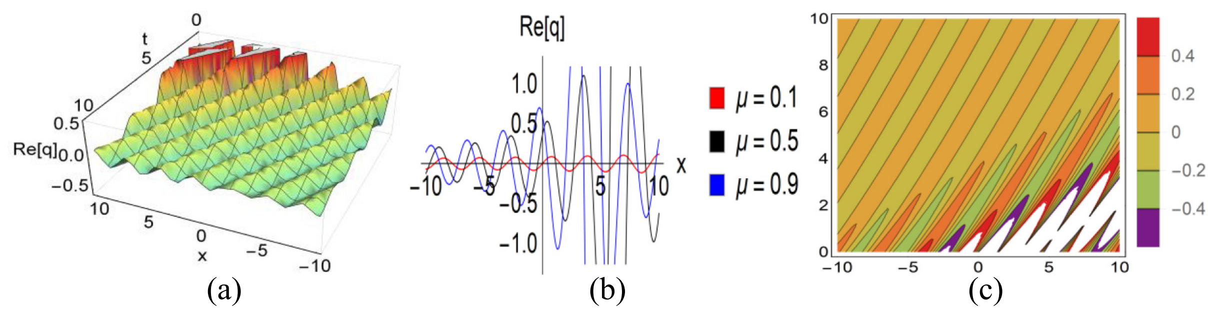

Fig. 7. (a) 3D plot, (b) 2D plot at $t = 3.5$, (c) contour plot of the real part of the solution (4.20).

7. Phase plane analysis

To proceed with phase plane analysis for the time-fractional unstable nonlinear Schrödinger Eq. (1.1), we introduce $X = u, Y = X'$. Now we may re-write Eq. (4.2) as a first-order dynamical system of the form,

$$\begin{cases} \frac{dX}{d\xi} = Y, \\ \frac{dY}{d\xi} = \frac{p^2+2\gamma+\nu}{k^2} X - \frac{2\eta}{k^2} X^3, \end{cases} \tag{7.1}$$

which defines the well-known phase plane associated with travelling wave solutions of the studied equation. $(X(\xi), Y(\xi))$ is the solution of the system (7.1).

The ordinary differential equations in Eq. (7.1) come from the Hamiltonian function in Eq. (7.2), by using Hamilton canonical equations $\frac{dX}{d\xi} = X' = \frac{\partial H}{\partial Y}$ and $\frac{dY}{d\xi} = Y' = -\frac{\partial H}{\partial X}$, where H is a C^2 function.

$$H(X, Y) = \frac{Y^2}{2} - \frac{p^2 + 2\gamma + \nu}{2k^2} X^2 + \frac{\eta}{2k^2} X^4. \tag{7.2}$$

Theorem 6.1. *The values of the Hamiltonian function are conserved (constant) along solution curves.*

Proof. We can write $H'(X, Y) = H_X X' + H_Y Y'$.
Applying Hamilton canonical equations, we obtain

$$H'(X, Y) = H_X H_Y + H_Y \left(-H_X\right) = 0.$$

Which implies $H(X, Y) = constant(= h)$.

$$\text{Hence } H(X, Y) = \frac{Y^2}{2} - \frac{p^2 + 2\gamma + \nu}{2k^2} X^2 + \frac{\eta}{2k^2} X^4 = h, \tag{7.3}$$

where h is the constant of integration.

Hence a given solution curve of the system (7.1) must therefore be on a level curve of the Hamiltonian function $H(X, Y)$. Hence proved.

Three equilibrium points of the dynamical system (7.1) are $\left(\pm\sqrt{\frac{p^2+2\gamma+\nu}{2\eta}}, 0\right)$ and $(0, 0)$. For values of $p = 1, \gamma = 1, \nu = 1, \eta = 1$ and $k = 1$, the equilibrium points $(0, 0)$, $(-1.4142, 0)$ and $(1.4142, 0)$ represent a circle, saddle point, and saddle point, respectively (See Figs. 8 and 9). On the other hand, for the values of $p = 0.5, \gamma = -1.25, \nu = 1, \eta = -1.5$ and $k = 1$. the equilibrium points $(-7638, 0)$, $(0, 0)$ and $(0.7638, 0)$ represent saddle point, circle, and saddle point, respectively (See Figs. 10 and 11). From this analysis we can conclude that the dynamics of the system altered due to the change of values of the parameters.

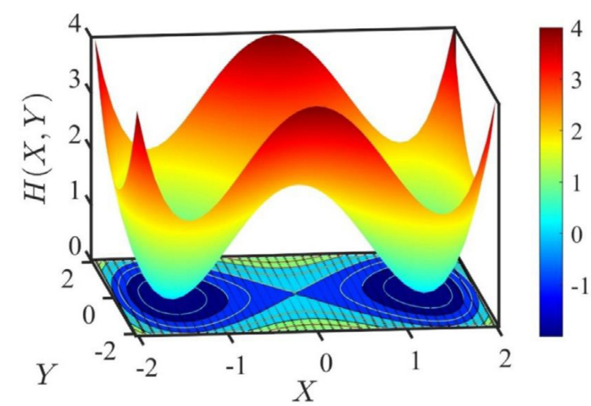

Fig. 8. Hamiltonian function $H(X, Y)$ of the Schrödinger equation corresponds to Eq. (7.2). Simulations were run for the values of $p = 1, \gamma = 1, \nu = 1, \eta = 1$ and $k = 1$.

8. Conclusions and future directions

In this study, we have successfully utilized an extended Kudryashov approach to investigate the time-fractional unstable nonlinear Schrödinger equation with a beta derivative. By employing this method, we were able to generate precise travelling wave solutions, including exponential, trigonometric, hyperbolic, and rational solutions. These solutions exhibit various shapes such as V-shaped, periodic, singular periodic, flat kink, and singular bell solitons, which are obtained for specific parameter values. Notably, these solutions are more general as

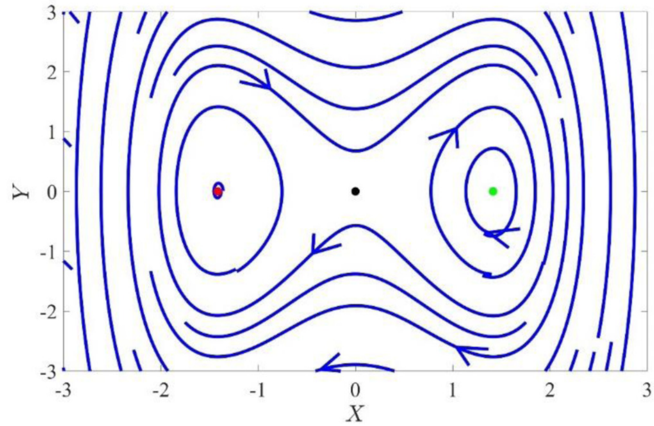

Fig. 9. Phase plane visualization of the system of ODEs (7.1) for the values of $p = 1, \gamma = 1, \nu = 1, \eta = 1$ and $k = 1$. Three equilibrium points are $(0,0), (-1.4142, 0)$ and $(1.4142, 0)$.

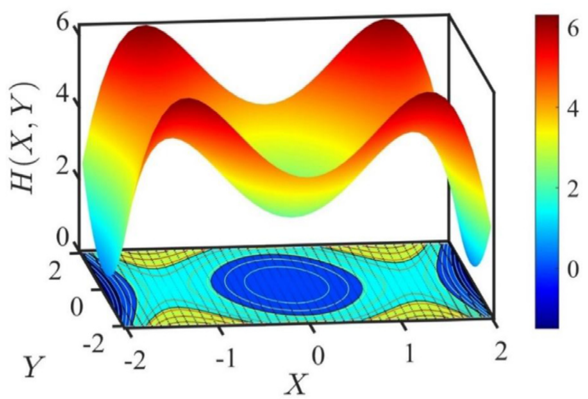

Fig. 10. Hamiltonian function $H(X,Y)$ of the Schrödinger equation corresponds to Eq. (7.2). Simulations were run for the values of $p = 0.5, \gamma = -1.25, \nu = 0.5, \eta = -1.5$ and $k = 1$.

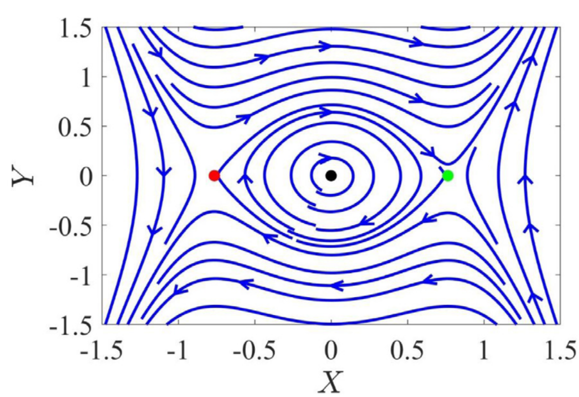

Fig. 11. Phase plane visualization of the system of ODEs (7.1) for the values of $p = 0.5, \gamma = -1.25, \nu = 0.5, \eta = -1.5$ and $k = 1$. Three equilibrium points are $(0,0)$, $(-7638, 0)$ and $(0.7638, 0)$.

they involve multiple free parameters. Therefore, the obtained travelling wave solutions have significant potential for practical applications in applied science and engineering.

Furthermore, our analysis demonstrates the effectiveness and conciseness of the extended Kudryashov method with the beta derivative. This suggests that it can be employed to extract soliton solutions from other fractional nonlinear Schrödinger equations (FNLEEs). After determining the Hamiltonian function, we briefly examined the phase plane and presented the graphical phase portrait of the system in Figs. 8–11. Through bifurcation analysis, we observed that altering the parameter values can lead to changes in the dynamics of the soliton solutions of the Schrödinger equation. This finding has important implications for optical fibres, nonlinear optics, and communication systems. It is worth mentioning that all the reported results in this article successfully satisfy the governing equation, ensuring the validity of our findings.

In this research paper, we present our findings based on the Ansatz method. It would be intriguing to explore alternative approaches for determining the solutions of the time-fractional Schrödinger equation and their applications in real-world situations. Specifically, in this study, we utilize Beta fractional derivatives to characterize the behaviour of the time fractional Schrödinger equation. While there are numerous studies available in the literature on the time-fractional Schrödinger equation,[14,43] limited efforts have been devoted to comprehending the fractional differential effects of other variables in specific situations.

Declaration of competing interest

The authors declare that they have no known competing financial interests or personal relationships that could have appeared to influence the work reported in this paper.

Data availability

No data was used for the research described in the article.

References

1. Rehman HU, Awan AU, Allahyani SA, Tag-ElDin EM, Binyamin MA, Yasin S. Exact solution of paraxial wave dynamical model with Kerr Media by using ϕ^6 model expansion technique. *Results Phys*. 2022;42:105975, 13.
2. Rehman HU, Awan AU, Tag-ElDin EM, Alhazmi SE, Yassen MF, Haider R. Extended hyperbolic function method for the (2+1)-dimensional nonlinear soliton equation. *Results Phys*. 2022;40:105802, 6.
3. Rehman HU, Awan AU, Habib A, Gamaoun F, Tag El Din EM, Galal AM. Solitary wave solutions for a strain wave equation in a microstructured solid. *Results Phys*. 2022;39:105755, 10.
4. Liu JG, Osman MS. Nonlinear dynamics for different nonautonomous wave structures solutions of a 3D variable-coefficient generalized shallow water wave equation. *Chinese J Phys*. 2022;77:1618–1624.
5. Gorenflo R, Mainardi F. *Fractional Calculus: Integral and Differential Equations of Fractional Order, Vol. 1997*. Vienna: Springer; 1997:223–276.
6. Mahiuddin M, Khan MIH, Pham ND, Karim MA. Development of fractional viscoelastic model for characterizing viscoelastic properties of food material during drying. *Food Biosci*. 2018;23:45–53.
7. Podlubny I. *Fractional Differential Equations an Introduction to Fractional Derivatives, Fractional Differential Equations, to Methods of Their Solution and Some of Their Applications*. San Diego: Academic Press; 1998.
8. Park C, Nuruddeen RI, Ali KK, Muhammad L, Osman MS, Baleanu D. Novel hyperbolic and exponential Ansatz methods to the fractional fifth-order Korteweg–de Vries equations. *Adv Differ Equ*. 2020;2020(1):1–2.
9. Siddique I, Jaradat MM, Zafar A, Mehdi KB, Osman MS. Exact traveling wave solutions for two prolific conformable M-fractional differential equations via three diverse approaches. *Results Phys*. 2021;28:104557, 15.
10. Djennadi S, Shawagfeh N, Osman MS, Gómez-Aguilar JF, Arqub OA. The tikhonov regularization method for the inverse source problem of time fractional heat equation in the view of ABC-fractional technique. *Phys Scr*. 2021;96(9):094006, 17.
11. Nisar KS, Ciancio A, Ali KK, et al On beta-time fractional biological population model with abundant solitary wave structures. *Alex Eng J*. 2022;61(3):1996–2008.
12. Cao Y, Dhahad HA, Jarad F, et al Extracting novel categories of analytical wave solutions to a nonlinear Schrödinger equation of unstable type. *Results Phys*. 2021;31:105036, 14.
13. Bhrawy AH, Abdelkawy MA, Biswas A. Optical solitons in (1+1) and (2+1) dimensions. *Optik*. 2014;125(4):1537–1549.
14. Ilie M, Biazar J, Ayati Z. Analytical study of exact traveling wave solutions for time-fractional nonlinear Schrödinger equations. *Opt Quantum Electron*. 2018;50(12):1–3.
15. Galati L, Zheng S. Nonlinear Schrödinger equations for Bose–Einstein condensates. *AIP Conf Proc*. 2013;1562(1):50–64.

16. Copie F, Randoux S, Suret P. The physics of the one-dimensional nonlinear Schrödinger equation in fiber optics: Rogue waves, modulation instability and self-focusing phenomena. *Rev Phys*. 2020;5:100037, 17.
17. Demiray S, Ünsal Ö, Bekir A. New exact solutions for Boussinesq type equations by using $(G'/G, 1/G)$ and $(1/G')$-expansion methods. *Acta Phys Pol A*. 2014;125(5):1093–1098.
18. Wazwaz AM. Multiple-soliton solutions for the KP equation by Hirota's bilinear method and by the tanh–coth method. *Appl Math Comput*. 2007;190(1): 633–640.
19. Aktar MS, Akbar MA, Osman MS. Spatio-temporal dynamic solitary wave solutions and diffusion effects to the nonlinear diffusive predator–prey system and the diffusion-reaction equations. *Chaos Solitons Fractals*. 2022;160:112212.
20. Khan K, Salam MA, Mondal M, Akbar MA. Construction of traveling wave solutions of the (2+1)-dimensional modified KdV-KP equation. *Math Methods Appl Sci*. 2023;46:2042–2054.
21. Khan K, Akbar MA. Traveling wave solutions of the (2+ 1)-dimensional Zoomeron equation and the Burgers equations via the MSE method and the exp-function method. *Ain Shams Eng J*. 2014;5(1):247–256.
22. Yao SW, Islam ME, Akbar MA, Inc M, Adel M, Osman MS. Analysis of parametric effects in the wave profile of the variant Boussinesq equation through two analytical approaches. *Open Phys*. 2022;20(1):778–794.
23. Zheng B. A new Bernoulli sub-ODE method for constructing traveling wave solutions for two nonlinear equations with any order. *UPB Sci Bull Ser A*. 2011;73(3):85–94.
24. Ma YL, Li BQ, Fu YY. A series of the solutions for the Heisenberg ferromagnetic spin chain equation. *Math Methods Appl Sci*. 2018;41(9):3316–3322.
25. Abuasad S, Hashim IS. Homotopy decomposition method for solving higher-order time-fractional diffusion equation via modified beta derivative. *Sains Malays*. 2018;47(11):2899–2905.
26. Akbar MA, Akinyemi L, Yao SW, et al Soliton solutions to the Boussinesq equation through sine-Gordon method and kudryashov method. *Results Phys*. 2021;25:104228, 10.
27. Awan AU, Rehman HU, Tahir M, Ramzan M. Optical soliton solutions for resonant Schrödinger equation with anti-cubic nonlinearity. *Optik*. 2021;227:165496, 10.
28. El-Borai MM, El-Owaidy HM, Ahmed HM, et al Topological and singular soliton solution to Kundu–Eckhaus equation with extended Kudryashov's method. *Optik*. 2017;128:57–62.
29. Nisar KS, Ilhan OA, Abdulazeez ST, Manafian J, Mohammed SA, Osman MS. Novel multiple soliton solutions for some nonlinear PDEs via multiple exp-function method. *Results Phys*. 2021;21:103769, 10.
30. Malik S, Almusawa H, Kumar S, Wazwaz AM, Osman MS. A (2+ 1)-dimensional Kadomtsev–Petviashvili equation with competing dispersion effect: Painlevé analysis, dynamical behavior and invariant solutions. *Results Phys*. 2021;23:104043, 8.
31. Awan AU, Tahir M, Abro KA. Multiple soliton solutions with chiral nonlinear Schrödinger's equation in (2+ 1)-dimensions. *Eur J Mech-B/Fluids*. 2021;85:68–75.
32. Ma WX. Soliton solutions by means of Hirota bilinear forms. *Partial Differ Equ Appl Math*. 2022;5:100220, 5.
33. Ma WX. N-Soliton solutions and the Hirota conditions in (2+1)-dimensions. *Opt Quantum Electron*. 2020;52:511. 12.
34. Ismael HF, Sulaiman TA, Nabi HR, Mahmoud W, Osman MS. Geometrical patterns of time variable Kadomtsev–Petviashvili (I) equation that models dynamics of waves in thin films with high surface tension. *Nonlinear Dynam*. 2023;111(10):9457–9466.
35. Razzaq W, Zafar A, Ahmed HM, Rabie WB. Construction solitons for fractional nonlinear Schrödinger equation with β-time derivative by the new sub-equation method. *Ocean Eng Sci*. 2022. http://dx.doi.org/10.1016/j.joes.2022.06.013, [in press].
36. Lu D, Seadawy A, Arshad M. Applications of extended simple equation method on unstable nonlinear Schrödinger equations. *Optik*. 2017;140:136–144.
37. Tala-Tebue E, Djoufack ZI, Fendzi-Donfack E, Kenfack-Jiotsa A, Kofané TC. Exact solutions of the unstable nonlinear Schrödinger equation with the new Jacobi elliptic function rational expansion method and the exponential rational function method. *Optik*. 2016;127(23):11124–11130.
38. Raheel M, Bekir A, Tariq KU, Cevikel A. Soliton solutions to the generalized (1+1)-dimensional unstable space time-fractional nonlinear Schrödinger model. *Opt Quantum Electron*. 2022;54(10):1–5.
39. Atangana A, Baleanu D, Alsaedi A. Analysis of time-fractional Hunter-Saxton equation: A model of neumatic liquid crystal. *Open Phys*. 2016;14(1): 145–149.
40. Siddique I, Mirza AM, Shahzadi K, Akbar MA, Jarad F. Diverse precise traveling wave solutions possessing beta derivative of the fractional differential equations arising in mathematical physics. *J Funct Spaces*. 2022;2022:5613708, 13.
41. Al-Amin M, Islam MN, Akbar MA. Adequate wide-ranging closed-form wave solutions to a nonlinear biological model. *Partial Differ Equ Appl Math.*. 2021;4:100042, 7.
42. Özkan EM, Özkan A. The soliton solutions for some nonlinear fractional differential equations with Beta-derivative. *Axioms*. 2021;10(3):203. 15.
43. Wang G, Xu T. Optical soliton of time fractional Schrödinger equations with He's semi-inverse method. *Laser Phys*. 2015;25(5):055402, 8.